JOINT EUROPEAN TORUS

JET–P(90)59

M.von Hellermann, W. Mandl, H.P. Summers, A. Boileau, J.Frieling
and JET Team

Investigation of Thermal and Slowing Down Alpha Particles on JET using Charge Exchange Spectroscopy

"This document contains JET information in a form not yet suitable for publication. The report has been prepared primarily for discussion and information within the JET Project and the Associations. It must not be quoted in publications or in Abstract Journals. External distribution requires approval from the Publications Officer, JET Joint Undertaking, Abingdon, Oxon, OX14 3EA, UK".

"Enquiries about Copyright and reproduction should be addressed to the Publications Officer, EFDA, Culham Science Centre, Abingdon, Oxon, OX14 3DB, UK."

The contents of this preprint and all other JET EFDA Preprints and Conference Papers are available to view online free at www.iop.org/Jet. This site has full search facilities and e-mail alert options. The diagrams contained within the PDFs on this site are hyperlinked from the year 1996 onwards.

Investigation of Thermal and Slowing Down Alpha Particles on JET using Charge Exchange Spectroscopy

M.von Hellermann, W. Mandl, H.P. Summers, A. Boileau[1], J.Frieling[2]
and JET Team*

JET-Joint Undertaking, Culham Science Centre, OX14 3DB, Abingdon, UK

[1]Tokamak de Varennes, Varennes, Quebec, Canada.
[2]FOM Instituut voor Atoom-en Molecuulfysica Amsterdam, The Netherlands
** See Appendix 1*

Preprint of Paper to be submitted for publication in
Plasma Physics and Controlled Fusion

ABSTRACT.

Thermal alpha particles are observed in JET during helium discharges using spectral emission in He II (n=4→3) near 4685Å following charge transfer reactions along the path of the neutral deuterium heating beams. New and reappraised He^{+2} /H charge transfer cross-sections are presented. The effects of cross-section energy dependence on temperatures, velocities and absolute densities deduced from thermal alpha particle charge exchange spectra are evaluated. The possibility of detecting fusion alpha particles produced at 3.5MeV and slowing-down by collisions with plasma electrons and ions using visible charge exchange spectroscopy is addressed. The spectral signature of slowing-down fusion alpha particles expected during the deuterium-tritium phase of JET is modelled and its identification against thermal alpha particle and background radiation is investigated.

1. Introduction

Observations of spectral emission from impurity ions in fusion plasmas following charge transfer from neutral deuterium or hydrogen beams has made great impact on deduction of impurity ion temperature, plasma rotation and ion density in recent years. The reactions are

$$X^{(+z_o)} + D^{(o)}_{beam}(1s) \rightarrow X^{(+z_o-1)}(n\ell) + D^{+}$$
$$X^{(+z_o-1)}(n\ell) \rightarrow X^{(+z_o-1)}(n'\ell') + h\nu \qquad (1)$$

where $X^{(+z_o)}$ is a fully ionised impurity ion of nuclear charge z_o. In JET, transitions n→n' in the visible spectral region $\lambda > 4000$Å are observed and the fast neutral source $D^{(o)}$ is the heating beams with primary particle energy in the range 40 - 80 keV/amu. It is to be noted that restriction to visible transitions will be essential for the active phase of JET as the collected light can be transferred by radiation resistant optical fibres to a remote diagnostic hall. Such measurements are intrinsically spatially resolved since the intersection of a line of sight and the neutral beams defines a well localized observation volume.

The experimental arrangements, diagnostic methodology and deductions of JET behaviour have been described previously . [Boileau et al. (1989), von Hellermann et al. (1990)].In this paper, attention is focussed specifically on He II (n=4-3) emission near $\lambda = 4685$Å. The spectral characteristics of the beam driven feature are usually recovered from the composite spectrum which includes edge features and bremsstrahlung radiation using a multi-gaussian fit procedure. Ion temperature and bulk plasma rotation velocity are deduced respectively from the spectral line width and position of the charge exchange component using a non-rotating edge line as reference. We wish to explore the validity of these deductions when the He^{+2} temperature is very high (> 20 keV). That this is a relevant question stems from the fact that $v\sigma$ where σ is the effective emission cross-section for He II (n=4-3) is not constant with relative speed v of the colliding He^{+2} and D^{o}. The monoenergetic effective emission coefficient $v\sigma$ is peaked at $v \sim 1.4$ at.u. (N.B. the atomic unit of speed is equivalent to ~ 25 keV /amu) falling steeply at higher speeds and less steeply at lower speeds. This can cause an asymmetric and displacéd emission line profile depending upon observational line of sight orientation relative to the neutral beams.

The second issue is detection of alpha particles produced by deuterium-tritium fusion in a reacting plasma. Future plans for JET include a final 'active' phase in which fuelling will be with a 50% mixture of deuterium and tritium. A thermonuclear power production to input power ratio $Q_{D\text{-}T}$ ~1 is anticipated which will imply an alpha particle power of ~ 5 MW. The alpha particles are born at 3.5 MeV and slow by collisions with electrons down to a critical speed v_o (~ 100 keV) at which point ion collisions become important. The slowing down time is ~ 1 sec. A range of alpha particle diagnostics have been under study in recent years. One class is based on exploiting the charge transfer reaction through use of appropriate diagnostic neutral beams. Single charge transfer with associated emission of cascade radiation or double charge transfer with energy analysis of escaping neutralised alpha particles are both possibilities. Detection of alpha particles at their birth energy by charge exchange requires a probing beam with particle velocities matching the alpha particle velocity. The neutral particle current density (~ 0.5 A/cm^2) at 880 keV/amu, corresponding to a neutral particle density of 10^9 cm^{-3} in the centre of the plasma, which would be required to detect alpha particles, unlikely to be available in the lifetime of JET. This paper is concerned with the feasibility of detecting He II (n=4-3) emission from alpha particles following charge exchange with neutral deuterium in the existing JET heating beams. The parameters of the beam heating system are presently upgraded to 140keV at 30 A and a detailed programme based on 160 keV ^{3}He injection is being prepared. Such beam particle energies allow significant interaction with slowed alpha particles with energies < 200 keV/amu. We are concerned with the magnitude and spectral profile of the resulting He II (n=4-3) emission. The restriction of the highest detectable alpha particle energies is associated with the steep fall of the effective emission coefficient with relative collision speed. This also restricts the Doppler half width of the emission feature to < 50Å and so allows the possibility of discrimination against a thermal bremsstrahlung background.

Evidently detailed knowledge of the charge exchange cross-sections and especially the state selective partial cross-sections for $n\ell$ shells with $n \geq 4$ are essential. We have conducted detailed investigations in collaboration with the experimental group at Groningen (FOM-KVI) and Amsterdam (FOM-AMOLF) which are summarised in Section 2. In Section 3, modelling of effective emission for Maxwellian distributions is considered. In this Section detailed results and corrections to ion temperature, density and rotation at high temperatures are presented. In Section 4, the feasibility of alpha particle

detection in JET is addressed. This is concerned with the alpha particle power required for a spectroscopic measurement via He II (n=4-3) emission. Detailed predictions of the power likely to be achieved in JET are not the subject of this work. The conclusions are in Section 5.

2. Charge Exchange Data for He^{+2}

Cross-section data for the fundamental charge transfer reaction $He^{+2} + D(1s) \rightarrow He^{+}(n\ell) + D^{+}$ are the starting point for calculation of effective emission coefficients. Also these cross-sections contribute to the attenuation of neutral deuterium beams along with ionising collisions and similar processes with deuterons and other impurities in the plasma. For charge exchange σ_{tot}, σ_n and $\sigma_{n\ell}$ are all required and the complete energy range relevant to fusion plasmas is 500 eV/amu $\leq E \leq$ 880 keV/amu.

σ_{tot} Principal sources of experimental measurements are Nutt et al. (1978), Shah & Gilbody (1978) and Hvelplund & Anderson (1982) which collectively span the range 500 eV/amu $\leq E \leq$ 500 keV/amu. They form a self consistent data set. The Hvelplund & Anderson values are normalised to those of Shah & Gilbody at 75 keV/amu, a procedure supported within their experimental error bars by separate calibration checks. The data with representative error bars are shown in Figure 1. The older experimental data of Olson et al. (1977) are not shown but are generally larger (at most 25% at E = 40 keV/amu). There are available to us, four comprehensive theoretical calculations, namely, Belkic et al. (1987, 1991), Ryufuku (1982), Olson (1988) and Fritsch (1988, 1989) (see also our acknowledgements) which include σ_n and $\sigma_{n\ell}$ decomposition. The theoretical σ_{tot} values of Belkic and Fritsch are plotted in Figure 1. The Belkic data (in the boundary corrected Born approximation) are valid in the high energy region and agree closely with experimental data. The elaborate close-coupled atomic orbital calculations of Fritsch encompass the whole medium and low energy regions and also show close agreement with experiment. The data of Ryufuku (1982) has been adopted by us in earlier work, while the classical Monte Carlo calculations of Olson (1977) have been widely used in fusion studies but show poorer agreement with the relevant experimental data.

As part of helium studies for JET, new optical measurements of state selective charge exchange cross-sections have been carried out by Hoekstra (1990) (0.3 keV/amu $\leq E \leq$ 13 keV/amu) and are in progress by Frieling et al. (1991)

(60 keV/amu ≤ E ≤ 120 keV/amu). The collision studies are made for the cross-sections of the He^{+1} n=4, ℓ states. In addition the data of Hoekstra include σ_{2p} for 0.3 keV/amu ≤ E≤ 1.75 keV/amu and $\sigma_{2p,\,3p,\,4p}$ for 2.5 keV/amu < E < 13 keV/amu. Hoekstra has shown by making use of the equation

$$\sigma_{tot} = \sum_{n} \sigma_{np} + \sigma_{2s} \qquad (2)$$

that his optical measurements agree within ~ 7% with the total charge exchange data of Gilbody's group. This is when the σ_{2s} cross-section experimentally determined by Shah and Gilbody (1974, 1978) is added to his results. Hoekstra's data, prepared in this manner between 2.5 keV/amu ≤ E ≤ 13 keV/amu are shown in Figure 1. At lower energies σ_{2p} is almost equal to σ_{tot}. The preferred data for σ_{tot} adopted in the JET data base is the heavy solid curve, based on the experimental data of Gilbody's group, Hoekstra and theory of Fritsch and Belkic. Experimental error bars suggest an expected error ≤ ±15% for 650 eV/amu ≤ E ≤ 550 keV/amu, while all data within their region of validity are bounded by ±25%. Partial cross-sections σ_n and $\sigma_{n\ell}$, shown next, are normalised to this curve.

σ_n The upper shell for the He II (n=4-3) transition, that is n=4, is subdominant for charge transfer from $D^{(o)}(1s)$. (The dominant shell is n_{crit}=2). Also charge exchange data for shells n>4 are necessary in the present application since the decrease with n of σ_n can be slow and so cascading significant. Calculation of capture to high subdominant shells is clearly difficult. Discrepancies between different methods become large and there is not at present an obvious basis for judgement. We wish to consider this point and begin with the empirical assumption that $\sigma_n \sim c\, n^{-\beta(E)}$ for high subdominal levels n > 4 where c is a constant. β = 3 arises in high energy approximations based on the available density of excited states in a hydrogen-like ion. We seek to choose $\beta(E)$ so that extrapolation of σ_n to higher n shells, for which there are no explicit data, may be performed. A value of $\beta(E)$ can be obtained by fitting the above expression to data in the interval [n,n-1] for some n. β in fact varies with n as well as E and this is shown in figure 2. From the various theoretical sources, the range of variation of β with n is shown as error bars, with the β value at the highest available n, ($\bar{n}$), marked with a symbol. The range of β corresponds to $\bar{n}$ to $\bar{n}$- 2. There is a general trend to $\beta \sim 3$ in the high energy region and a tendency for β to increase at lower energy. The latter is because the process becomes more state selective

and, due to the potential curve crossing mechanism, one n-value dominates with respect to electron capture. At high energy such a selectivity related to potential curve crossing does not exist.

Further interpretation of figure 2 cannot be secure without additional clarifying calculations - we only make some speculations. The low values of β and their small variation for the data of Belhic at $E < 50$ keV/amu perhaps imply a high energy based constraint on β in the calculations. The variation in β and especially the increasing value with n for the data of Olson for 60 keV/amu $< E <$ 100 keV/amu is surprising but may be due to counting statistics in the Monte Carlo method as the total cross-section falls with energy. The data of Fritsch shows the most striking variation of β. The trend is of a decreasing β with n and β for $n = 5$ is close to that of Ryufuku at energies 10 keV/amu $< E <$ 30 keV/amu. Decrease of β towards 3 at very high n is sometimes suggested, but there are some surprising values such as at 50 keV/amu and the trend is not smooth. Observation of the He II (n = 7-4) charge exchange spectroscopic line could be interesting in this context, but is unfortunately influenced by secondary ionizing collisions from the $n = 7$ level at JET tokamak densities.

For the JET data base, at present, we have adopted the β curve shown in heavy solid line, based on $n = 5$, for extrapolation in n. Retrospectively, the experimental data of Hoekstra (1990) were found to agree closely with this curve and are shown in figure 2 also. Note that these are for $\bar{n} = 4$.

By using the preferred β, $\sigma_{n=6}$ can be obtained by extrapolation from $n = 5$. The variation in β from figure 2 results in a variation in $\sigma_{n=6}$ which we view as the uncertainty in $\sigma_{n=6}$. Results on σ_n/σ_{tot} are summarised in Figure 3. The new experimental data of Hoekstra for n=4 are shown in this figure together with the older data of Ciric et al. (1985) for $n = 3$. Note that these data do not follow the detailed shape of the Fritsch data although the absolute values are in broad agreement. The JET preferred curves are shown in heavy solid line and are normalised to the preferred σ_{tot}, using the preferred β curve for extrapolation. Reliability of σ_n/σ_{tot} within $\pm 20\%$ for $n \leq 5$ for $E \geq 40$ keV/amu are expected but with significantly larger uncertainties at lower energies. Confidence in extrapolation in n at energies $E < 40$ keV/amu is evidently low in the light of the above discussion. New work is in progress on this point.

$\sigma_{n\ell}$ We concentrate on n=4 shell data. At tokamak densities and fields, ℓ-subshell populations are quite strongly mixed and so the ℓ distribution of direct charge exchange capture is less important. Data from different sources again show strong variation. For the JET database, we have sought a parametrisation of $\sigma_{n\ell}/\sigma_n$ data based on the observation that $\sigma_{n\ell}/\sigma_n$ rises with ℓ for $\ell<\ell_{crit}$ and then falls exponentially for $\ell>\ell_{crit}$ for some $\ell_{crit} \sim n_{crit}$. The parametrising is

$$\sigma_{n\ell}/\sigma_n = P_1\left[(2\ell+1)/(2\ell_{crit}+1)\right]^{P_2} \qquad \ell < \ell_{crit}$$

$$= P_1 e^{P_3\left(1-\ell_{crit}/\ell\right)} \qquad \ell > \ell_{crit} \qquad (3)$$

P_1 is a normalisation constant, $P_2 \sim 1$ and P_3 increases from - 1 to 2 between 1 keV/amu and 100 kev/amu. Best fits of P_1, P_2 and P_3 are obtained for each data source for n=4 at each density. Variations around these preferred values are quite large although trends are similar. Because of redistribution, the apparently large variation of the P_2 and P_3 parameters gives a variation of less than 5% in the effective emission coefficients at all relevant plasma conditions.

Preliminary results from Frieling et al. (1991) show excellent agreement with our preferred data for n=4 in the range 60 keV/amu$\leq E \leq$ 120 keV/amu.

$\sigma^{(eff)}_{n=4-3}$ The effective emission cross-sections for monoenergetic collisions are calculated for an extended range of energies and plasma conditions following the methods described in Boileau et al. (1989) using the preferred direct capture data described above. The results exhibit the range from no - to full-l-mixing and are computed from a proper model of plasma environment effects.

The monoenergetic effective emission coefficient for the He II (n=4-3) transition is shown in Figure 4 for typical plasma conditions. The observed charge exchange spectrum line profiles are the result of a convolution in velocity space of the He^{+2} velocity distribution function and the effective emission coefficient. The energy dependence of the coefficient acts as a sampling window whose width may be small compared to the total energy range of the He^{+2} particles, depending on their distribution function. The coefficient is a maximum at E = 50 keV/amu (v = 1.4 at.u.) falling with a full-width-half-maximum ~ 70 keV/amu (i.e. 0.8 at. u. $< v <$ 1.84 at.u.) and implies that He^{+2} ions with speeds relative to the $D^{(o)}_{beam}$ speed within the range 0.8 at.u $< v_{rel} <$ 1.84 at.u only

contribute significantly to the observed charge exchange emission signals. The anisotropic distribution of He^{+2} particles in velocity space matching the condition for maximum charge exchange emissivity leads generally to an asymmetric spectral profile. The anisotropy occurs when the direction of observation is not perpendicular to the direction of fast neutral beam particle propagation. We examine these effects for thermal and slowing down He^{+2} distribution functions.

3. Observation of Thermal Alpha Particles

The spectral environment in the vicinity of the He II (n=4→3) transition near 4685.2 Å is shown in Figure 5 in the absence of neutral beam injection, as measured during a discharge with $N_{He}/N_e \sim 20\%$. The helium signal is associated with line emission originating from the edge of the plasma. Two gaussians with temperatures typically of 50 eV to 100 eV and 300 eV to 700 eV are necessary to fit this signal adequately. These values are thought to be representative of the temperature range covered by the He II emission shell near the plasma boundary. The figure also shows the spectral ranges typically spanned by the red wing (long wavelength side) of the thermal and slowing-down fusion alpha particle features.

The composite spectrum includes several emission lines lying to the left of the He II line of interest and mainly due to low ionization stages of carbon (Figure 5 is representative of a carbon limiter plasma,with $Z_{eff} \sim 2$ largely due to carbon contamination). In a beryllium environment, the carbon lines are reduced, but the spectral interval is markedly altered by the occurrence of the Be II line at 4673.5 Å and of the Be IV line at 4658.5 Å. Such emission lines significantly restrict the spectral range available for alpha particle studies on the left hand side (blue wing) of the He II spectrum, leaving however the red wing intact. The hydrogen-like beryllium transition n=8→6 transition at 4685.2 Å coincident with the He II transition makes thermal alpha particle studies more difficult in a beryllium dominated machine, but does not restrict the spectral interval available for the study of slowing-down alpha particles as this line spans a smaller spectral range than the thermal alpha particle spectrum. It must also be stressed that beryllium may not be appropriate as a limiter material during deuterium - tritium experiments because of its large retention coefficient for hydrogen isotopes and the necessity to avoid a large tritium inventory in plasma facing structures. Figure 5 is thus a realistic representation of the spectral

environment of the He II (n=4→3) transition envisaged for alpha particle studies. It suggests that a line free spectral interval is available for alpha particle observation, mainly at > 4660 Å. If active impurity control with a pumped director on JET is realised in the future the effect of the CIV line near 4658.3 Å may also be considerably reduced.

The broadening of the He II line during neutral beam injection as a result of the additional high temperature charge exchange component is illustrated in Figure 6 (observation volume near the plasma centre viewed with a vertical line of sight; $T_{cx} \sim 4.7$ keV $\pm$ 0.2 keV). The spectral characteristics and amplitude of the thermal alpha component are routinely extracted from the composite spectrum using a multigaussian fit procedure. This technique may however not be appropriate for slowing down fusion alpha studies as their spectral profile is not expected to be gaussion in shape.

The alternative technique of background subtraction using a passive line of sight which does not intersect the neutral beams has been investigated. It has been used successfully to recover the thermal alpha particle signal down to the detection limit (Figure 7), in the spectral interval free of strong edge emission lines. The detection limit after subtraction of the background signal is imposed by the fluctuations of the bremsstrahlung level ϕ_{RMS}
It is expressed as

$$\phi_{RMS} = \left(\frac{2.\phi_{brems}.C}{\tau_{exp}} \right)^{1/2} \qquad (4)$$

where ϕ_{brems} is the continuum level, C is the overall calibration factor (in brightness per count rate) and τ_{exp} is the exposure time. Suppression of edge emission lines is not necessarily possible depending on toroidal asymmetries affecting the emission shells and the different geometries of the passive and active viewing lines. Thus it can be seen for example in Figure 7 that the signal below 1 keV still bears the signature of the strong edge He II component. There is a considerable spectral range where bremsstrahlung radiation is effectively eliminated and where the signal appearing above the detection limit is unambiguously attributed to the presence of alpha particles. The characteristics of the thermal alpha particle population deduced after background subtraction are in good agreement with those obtained from a multigaussian fit to the original composite spectrum.

Neutral beam modulation has also been used to recover small charge exchange signals severely contaminated by emission not originating from the active volume. In this case, a background spectrum collected during the small switch off time of the beams is subtracted from the composite spectrum bearing the active charge exchange signature. This technique yields convincing results for 100% beam modulation. It effectively suppresses the bremsstrahlung radiation and edge emission lines for spectra collected shortly before or after the neutral beam switch off interval, thus allowing charge exchange signals to be measured down to the detection limit expressed by eq. (3).

The temperature and toroidal rotation velocity (using tangential viewing) attributed to the thermal alpha particle features are affected by the energy dependence of the effective rate coefficient for the charge exchange reaction described by e.g. (1) Indeed, the effective rate coefficient varies with the relative velocity between the target alpha particle and the impacting fast neutral. The velocity of the thermal alpha particle along the neutral beam line must be added to the fast neutral velocity when evaluating the effective rate coefficient. This effect was first computed by von Hellermann et al. (1987) for several low-Z impurity ions. It results in a distortion of the observed spectral line which becomes more significant for greater Doppler widths (i.e. for larger temperatures or, at a given temperature, for ion species with a lower mass).

The change in effective full halfwidth and peak position (determining respectively the temperature and toroidal rotation velocity) depends on the neutral beam energy compared to the peak energy for charge exchange capture and the shape of the charge exchange rate coefficient over the thermal energy range corresponding to the full width of the maxwellian distribution. The relative position of the thermal maxwellian in velocity space with respect to the peak of effective rate coefficients is also a function of bulk plasma rotation. The angle of observation with respect to the neutral beam propagation axis determines whether the effective shift is seen as a red or a blue shift of the observed spectrum.

Similar calculation was more recently applied to UV charge exchange lines of carbon by Howell et al. (1988). Their calculation could not quite reconcile the velocity measurements obtained from two different geometries. The difference was used to stress the importance of relying on the proper effective rate

coefficients. Figures 8 therefore summarize the deviation in temperature, toroidal rotation velocity and effective rate coefficient presented in Figure 4 when the velocity dependent charge exchange cross-section and thermal distribution of target He^{+2} ions are taken into account. For the central viewing line of the JET multichord charge exchange spectroscopy viewing system, the distortion of the spectral line profile results in an apparent 13% decrease of the thermal alpha particle temperature at 15 keV. The effect on toroidal rotation velocity is significant for temperatures relevant to JET. Figure 8b indicates that an apparent velocity of ~ 7×10^4 m/s is expected in the case of a non-rotating 15 keV plasma, again for the central viewing line. This phenomenon also has a considerable impact on the thermal alpha particle density deduced from our measurements, with an apparent 27% decrease of the effective rate coefficient T_i ~ 15 keV. Equally important for the deduction of absolute alpha particle and other impurities absolute densities is the effect of $\sigma(E)$ averaged over a thermal distribution on the stopping cross-sections used for beam attenuation calculations. In light of the results presented in Figure 8c, such effect may have to be considered for high T_i plasmas when computing the fast neutral density in the observation volume, although the effect is not as pronounced for other target ions.

4. Spectral Signature of Slowing-Down Fusion Alpha Particles

The expected charge exchange line profile associated with fusion alpha particles is the result of a convolution in velocity space of the effective charge exchange rate coefficient presented in Figure 4 and the alpha particle slowing-down function $f_{sd}(V_\alpha)$ given by (Post et al., 1981)

$$f_{sd}(V_\alpha) = \left(\frac{S_\alpha \tau_{sd}}{4\pi}\right)\left(\frac{1}{V_c^3 + V_\alpha^3}\right) \qquad (4)$$

where S_α is the alpha particle source rate, τ_{sd} is the slowing-down time, V_α is the alpha particle velocity and V_c is a critical velocity depending on the electron temperature T_e [in keV].

$$V_c = 1.4 \times 10^8 \, T_e^{1/2}. \qquad (5)$$

For a plasma electron temperature of 15 keV (which determines V_c in the slowing alpha particle distribution function) a broad CX spectral profile with a width of approximately 150 Å is obtained due to the velocity selective charge exchange capture process. However, the amplitude and line shape are sensitive functions of observation angle and beam energy, as described in the previous section. At lower beam energies there are more alpha particles per velocity interval matching the velocity selective conditions but on the other hand the number of neutral particles is reduced because of increased attenuation. A further factor is the decreasing neutralization efficiencies of neutral injectors at high beam energies. Assuming constant neutral particle power at the source a maximum of effective signals is expected for a beam energy between 60 keV/amu and 80 keV/amu.

For moderate beam energies (E_{beam} = 60 keV/amu) there are relatively strong signals from the slowing-down particles. (Figure 9) The peak amplitude is comparable to the bremsstrahlung radiation level in the same wavelength interval. The spectral profile produced by the slowing-down alpha particles is rather flat with a slight slope in its plateau and a sharp drop-off at the wing. The characteristic features of the profile depend sensitively on the viewing angle, the assumed critical velocity and the neutral beam energy. In principle the slowing-down alpha particle distribution can be deconvolved and analysed provided the energy dependence of the charge exchange effective emission coefficient is known reliably, to yield the source rate and critical velocity.

Based on the thermal alpha particles measurements presented earlier and using the projected characteristics of the JET heating neutral beams during D-T operation, the expected signature of slowing down alpha particles and the absolute signal strength are computed. In this operation phase with up to 40 MW of ohmic and auxiliary heating, it is expected to achieve an alpha particle power level of up to 8 MW (with low to moderate electron densities $N_e < 5 \times 10^{19}$ m^{-3}, but high ion temperature $T_i > 15$ keV). If it is assumed that the mean alpha part particle density in the plasma centre is determined mainly by the production rate and the characteristic slowing-down time (~ 2s), that the main alpha particle production occurs within the q=1 surface and that outward diffusion can be neglected during the slowing-down process, then alpha particle densities in the plasma centre between 10^{17} m^{-3} and 10^{18} m^{-3} are expected. It is not our intention to present an accurate value for the expected alpha particle density in the plasma centre but to show that our diagnostic can detect what is nonetheless a realistic

estimate of the slowing-down alpha particle density. An example of a theoretical spectrum based on this estimate and consisting of the superposition of the thermal and slowing-down alpha particle contributions, as well as the continuum background radiation is shown in Figure 9a. The associated figure 9b shows the energy range of the detectable slowing down alpha particles. The absolute photon fluxes are based on an attenuation code used for the low-Z impurity calculations at JET [Boileau et al. (1989)] and the simulation uses the viewing geometry envisaged for fusion alpha particle studies on JET.

5. CONCLUSIONS

Charge exchange spectroscopy results on JET indicate that the spectral characteristics of a thermal alpha particle population can be recovered from a composite line spectrum. For spectral distributions well approximated by a gaussian shape, the temperature of the alpha particle population can be recovered conveniently by a multigaussian fit procedure. This is confirmed by the good agreement between the alpha particle temperature and other impurity temperatures observed in the vertical geometry where the energy dependence of the effective charge exchange rate coefficient is not expected to have a significant impact on the measured temperatures [Boileau et al. (1989)].

Background subtraction using a passive line of sight has been used successfully to recover charge exchange signals down to the detection limit imposed by bremsstrahlung radiation fluctuations. This approach allows observation of a charge exchange signal of complex spectral shape, as is expected for slowing-down fusion alpha particles. One advantage of this method over neutral beam modulation is that the two spectra (with and without charge exchange signals) are recorded simultaneously.

Measurement of the radial profile of a slowing-down alpha particle population by the JET charge exchange spectroscopy diagnostic has been assessed and appears to be feasible. The estimated signal-to-noise ratios depend critically on the concentration of alpha particles and the efficiency of background suppression. For so-called hot-ion mode plasmas with densities of about 5×10^{19} m^{-3} and alpha particle densities of the order of 10^{18} m^{-3} in the plasma centre, we expect charge exchange signals produced by slowing-down alpha particles of the same order of magnitude as the continuum radiation level. The latter is approximately 1 to 2 orders of magnitude above the detection limit. Alpha

particles with energies up to 400 keV should contribute to the charge exchange spectrum.

Acknowledgements

We are greatly indebted to Dr F de Heer and Dr R Hoekstra for much advice on collision cross-sections in this work.

We are also indebted to D Belkic, W Fritsch and R E Olson for communicating to us much more extended and detailed tabulations of their data than is available in the general literature. One of us (HPS) is on contract from the University of Strathclyde.

References

Boileau, A., von Hellermann, M. Horton, L.D., Spence, J., Summers, H.P., Plasma Phys.Contr. Fusion 31, 779 (1989).

Belkic, D., Saini, S. & Taylor, H.S. Phys Rev A 36, 1601 (1987).
Belkic, D. - Phys. Rev. - to be published (1991).
Ciric, D., Dijkkamp, D., Vlieg, E. and de Heer, F.J., J. Phys. B. 18, 4745 (1985).

von Hellermann, M.G. von, Mandl, W., Summers, H.P., Weisen, H., Boileau, A., Morgan, P.D., Morsi, H., Koenig, R., Stamp, M.F., Wolf, R., Rev. Sci. Instrum (1990) accepted for publication.

von Hellermann, M., Summers, H.P. Boileau, A & Horton, L.
Proc. of IAEA Large Tokamak Workshop on Ion Temperature Measurements, PPPL Princeton, N.J. (1987).

Frieling, J., Hoekstra, R. and de Heer, F.J. - J. Phys. B. - to be published (1991).

Fritsch, W., Phys. Rev. A38, 2664 (1988).

Fritsch, W., J. de Physique, 50 Coll. C1, 87 (1989).

Hoekstra, R. Ph.D. Thesis - Rijksuniversiteit Groningen (1990).

Hoekstra, R., Schlatmann, A.R., de Heer, F.J. and Morgenstern, R., J. Phys. B. 22, L 603 (1989).

Howell, R.B., Fonck, R.J., Knize, R.T., Jaehnig, K.P.,
Rev. Sci. Instrum. 59, 1521 (1988).

Hvelplund, P & Andersen, A., Physica Scripta 26, 375 (1982).

Nutt, W.L., McCullough, R.W., Brady, K., Shah, M.B. & Gilbody, H.B., J. Phys. B 11, 1457 (1978).

Olson, R.E., Salop, A., Phaneuf, R.A. & Meyer F.W., Phys Rev A14, 1867 (1977).

Olson, R.E. - private communication (1988).

Post, D.E., J. Fusion Energy 1, 129 (1981).

Ryufuku, H., Japan Atomic Energy Research Institute report.
JAERI - M - 82 - 031 (1982).

Shah, M.B. & Gilbody, H.B. J. Phys. B. 7, 630 (1974).

Shah, M.B. & Gilbody, H.B. J. Phys. B. 11, 121 (1978).

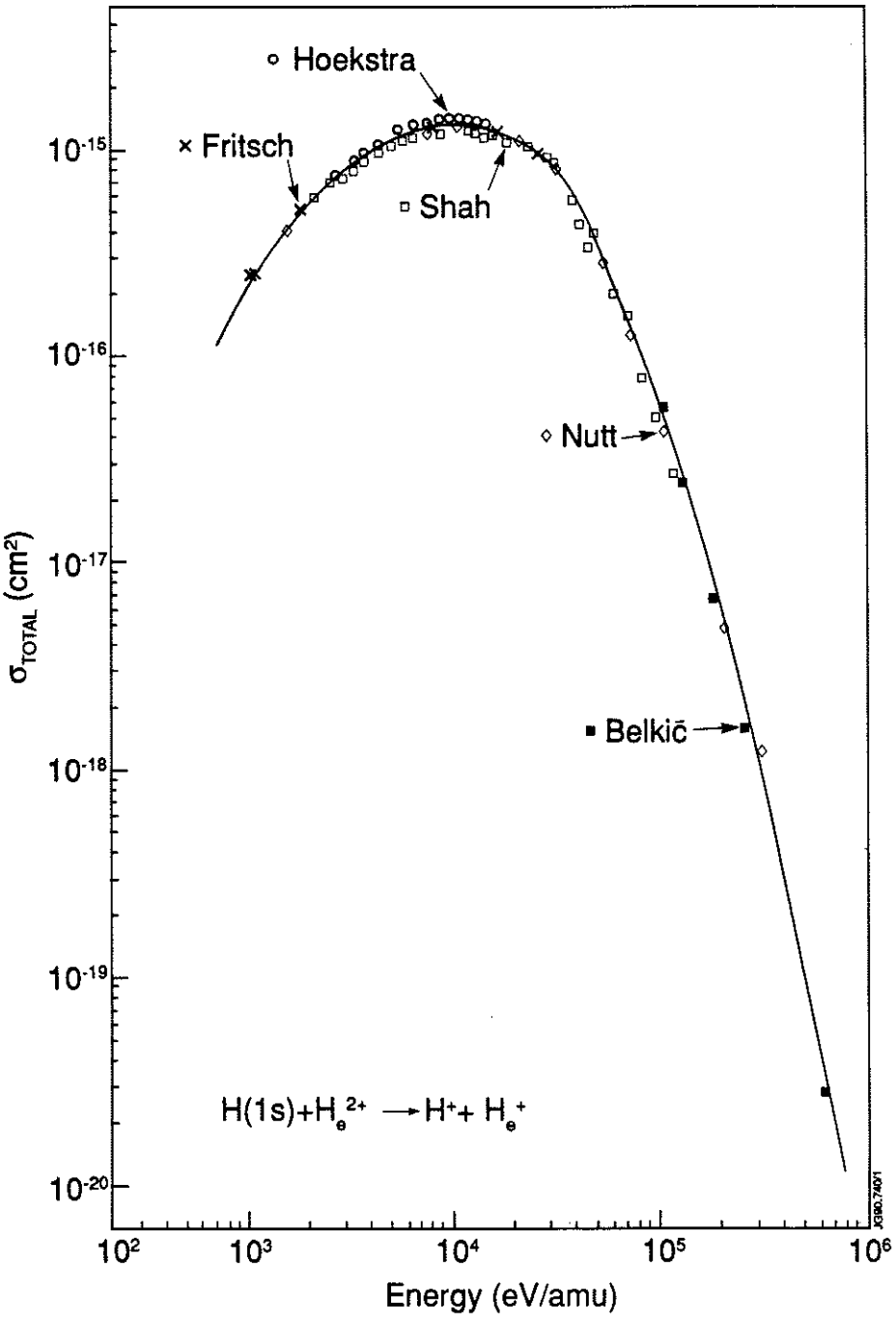

Figure 1 Comparison of different sources for σ_{tot} for the reaction $D(1s) + He^{+2} \rightarrow D^+ + He^+$. Preferred curve in heavy solid line.

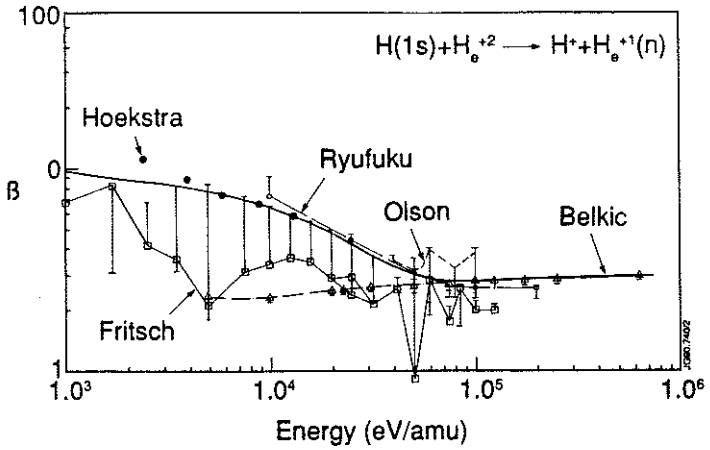

Figure 2 Comparison of β and its variation. β is obtained by fitting $\sigma_n = c\, n^{-\beta}$ at n and n-1 for some n.
Symbols mark β for $n = \bar{n}$ where $\bar{n}$ is the maximum available n in the data source. The error bars give the variation of β for $\bar{n}$, $\bar{n} - 1$, $\bar{n} - 2$ at fixed E.
O Ryufuku $\bar{n} = 5$; □ Fritsch $\bar{n} = 6$; + Olson $\bar{n} = 6$; × Belkic $\bar{n} = 7$;
• Experimental data of Hoekstra $\bar{n} = 4$.
Preferred curve in heavy solid line.

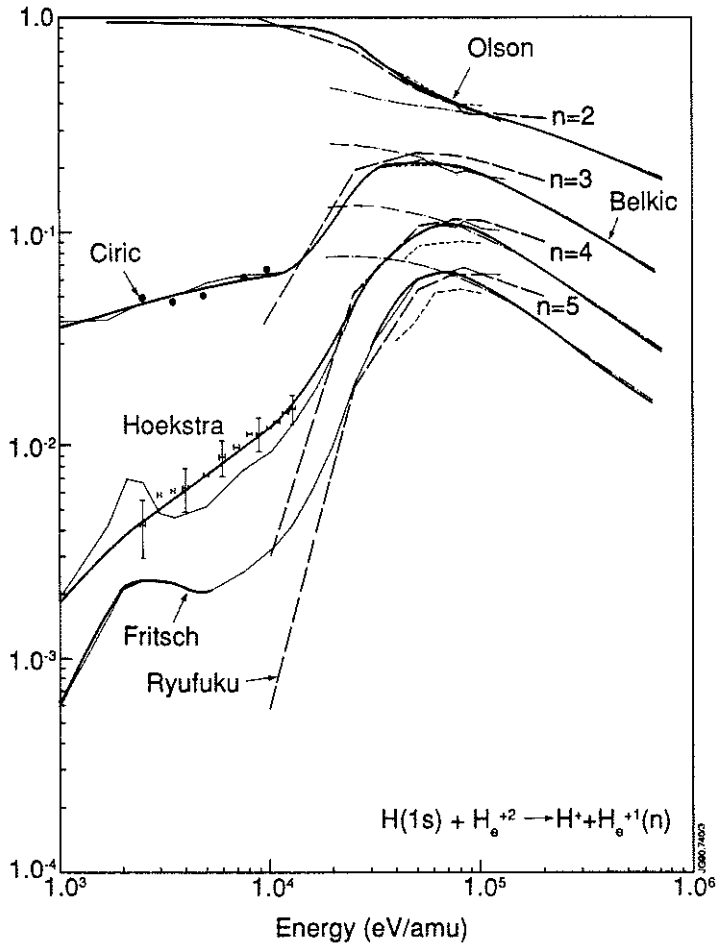

Figure 3 Comparison of σ_n/σ_{tot} for $n \leq 5$. σ_n/σ_{tot} error bars are derived from the uncertainty in β projection from n=5. Preferred curves in heavy solid line.

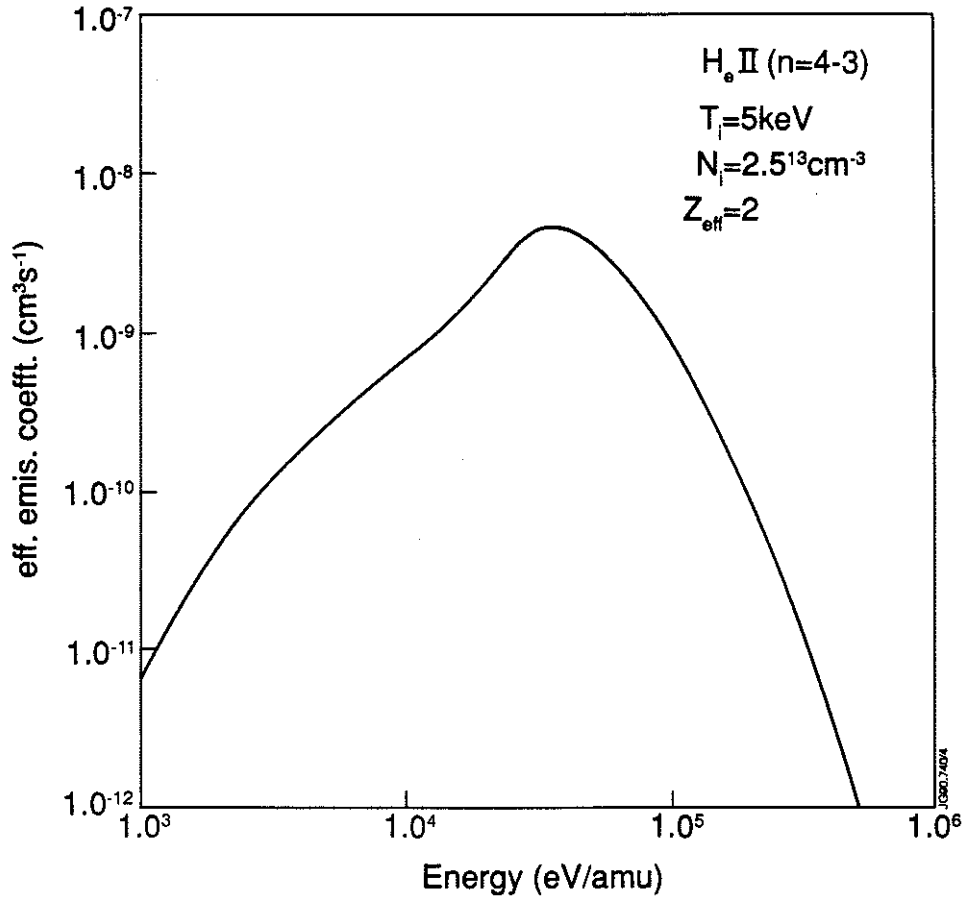

Figure 4 Effective emission coefficient for HeII (n=4-3) as a function of collision energy for $T_e = T_i = 5$ keV, $N_e = 2.0 \times 10^{19}$ m^{-3} $N_i = 1.0 \times 10^{19}$ m^{-3}, $Z_{eff} = 2$, $B_T = 3.0$ T.

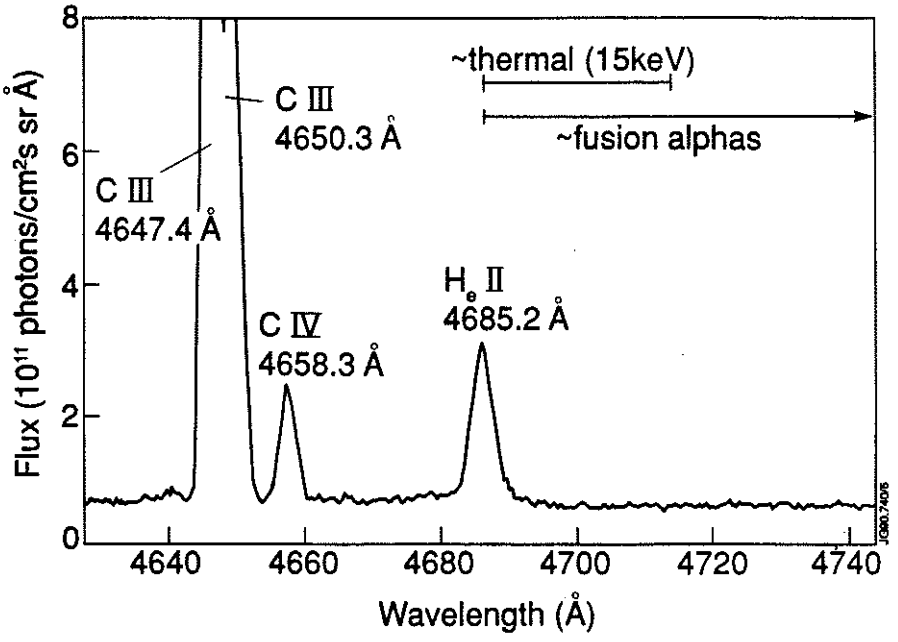

Figure 5 Spectral environment of He-II (n=4→3) line measured by a line of sight that does not intersect the neutral beams.

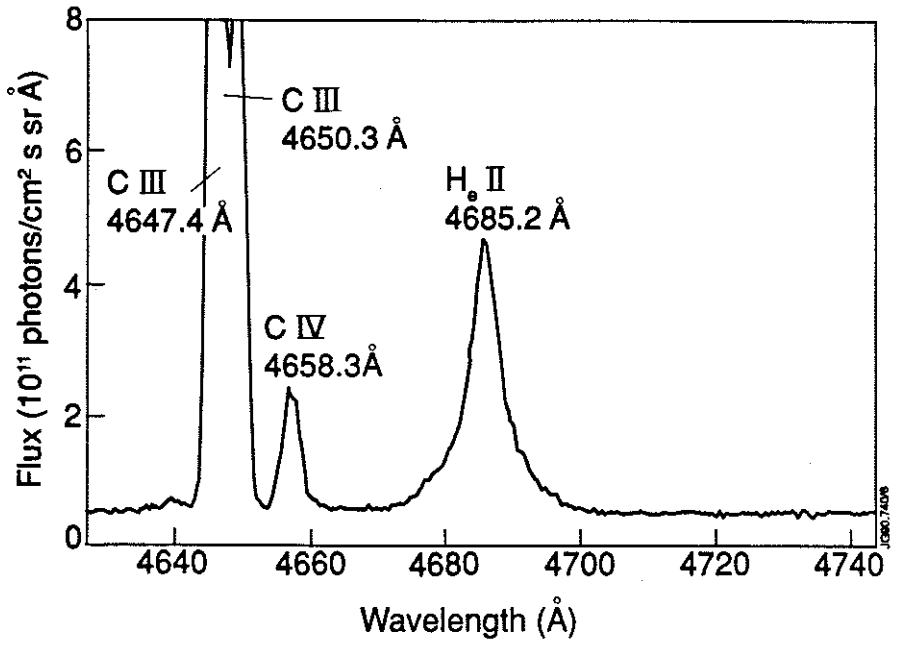

Figure 6 Same spectral range as in fig. 5 observed with a vertical viewing line crossing the neutral beams near the plasma centre. The CX feature appears mainly as a broadening of the composite He II line (T_i ~ 4.7 keV).

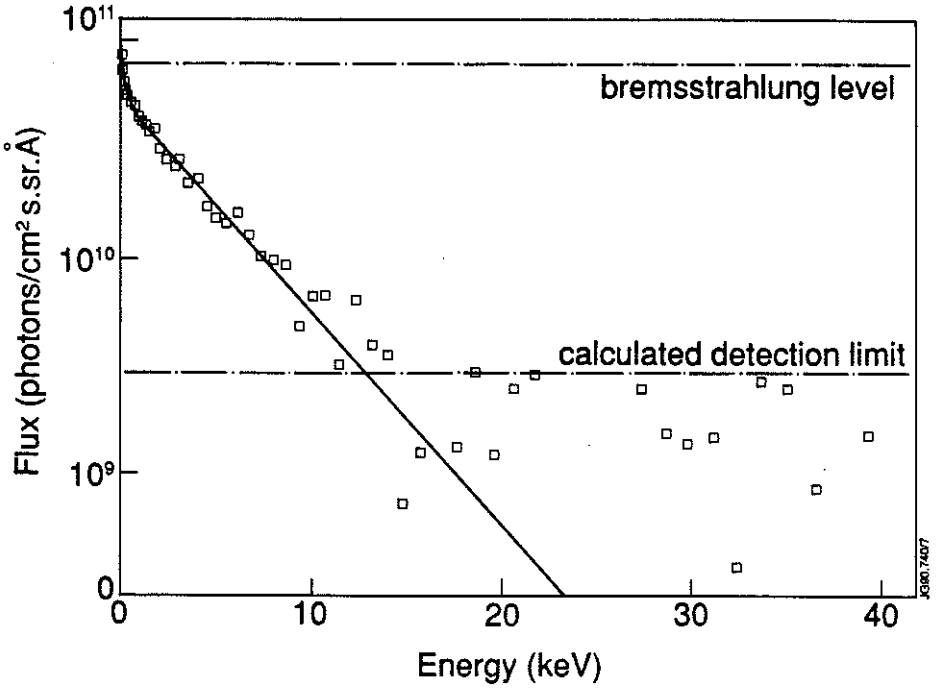

Figure 7 Red wing of the charge exchange helium spectrum plotted in the log (flux)/alpha particle energy plane to convert a gaussian shape into a straight line. This admittedly small signal was recovered down to the detection limit using a passive line of sight for background subtraction.

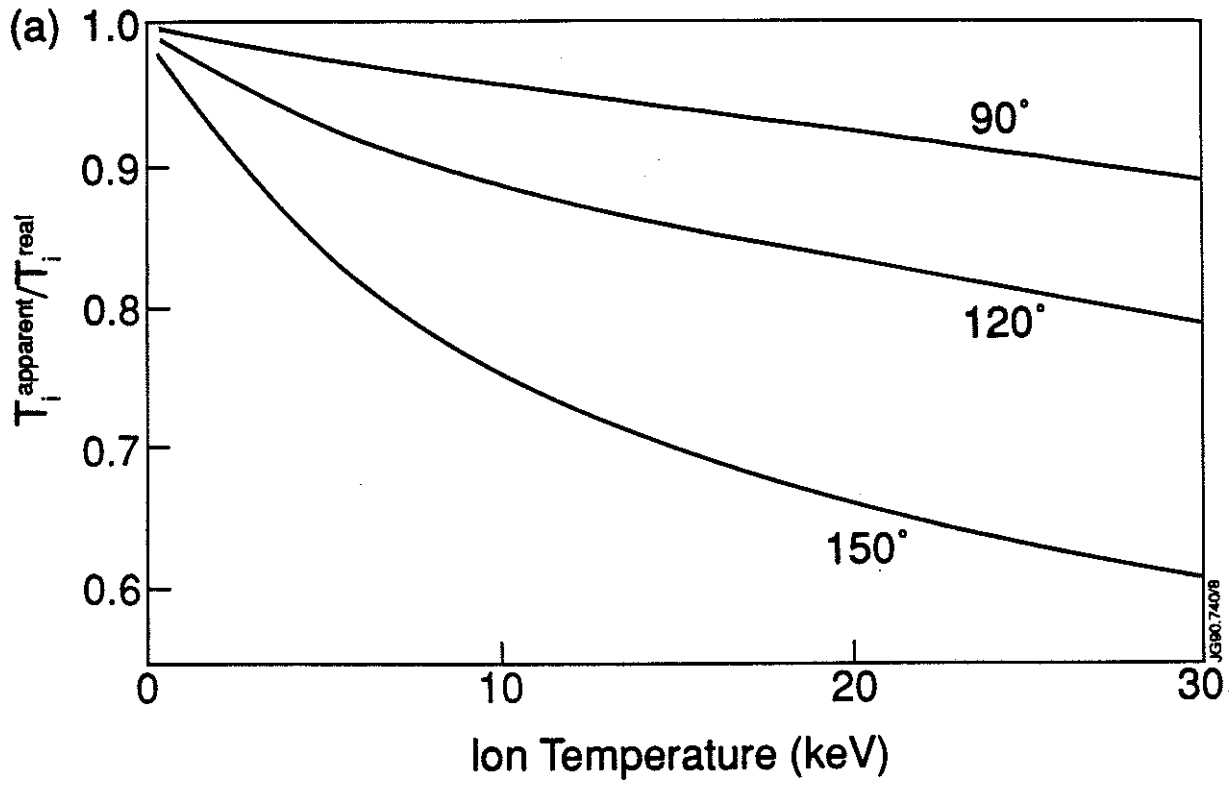
(a)
1.0
0.9
0.8
0.7
0.6
$T_i^{apparent}/T_i^{real}$
90°
120°
150°
0
10
20
30
Ion Temperature (keV)
JG90.740/8

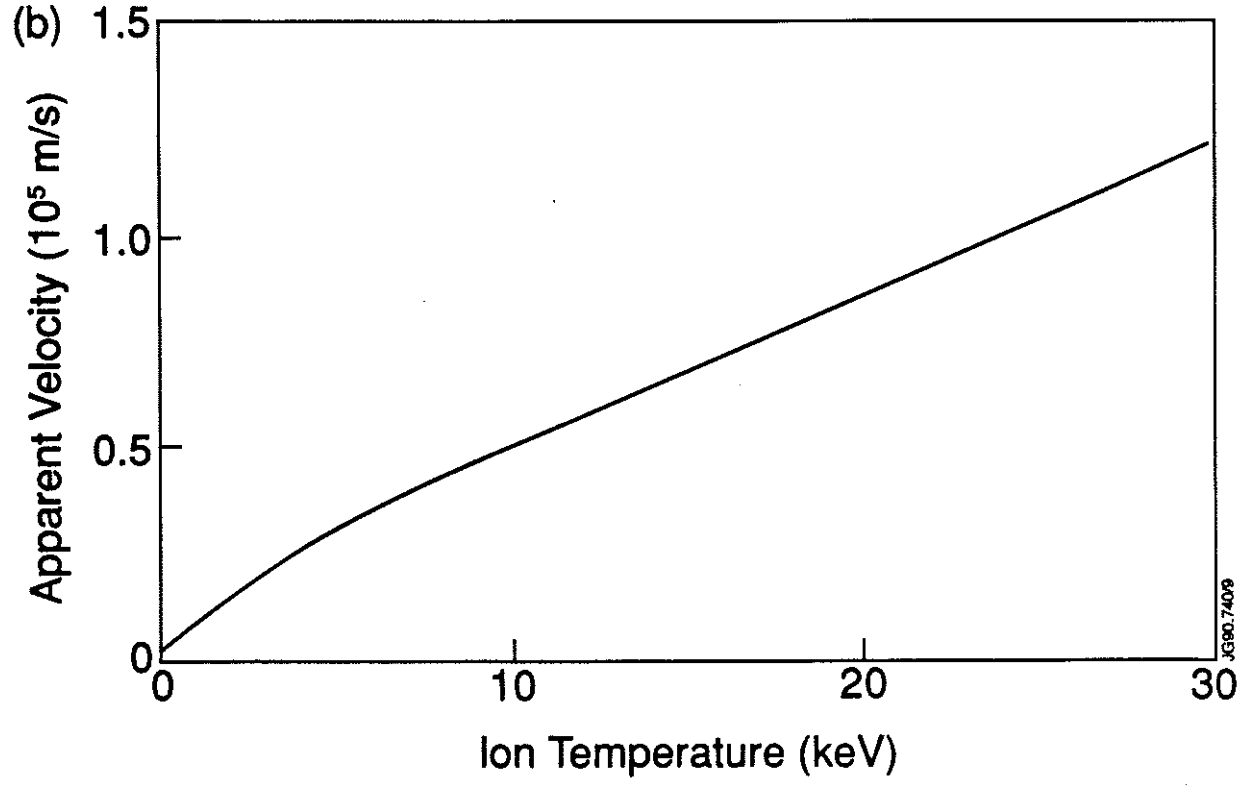
(b)
1.5
1.0
0.5
0
Apparent Velocity (10^5 m/s)
0
10
20
30
Ion Temperature (keV)
JG90.740/9

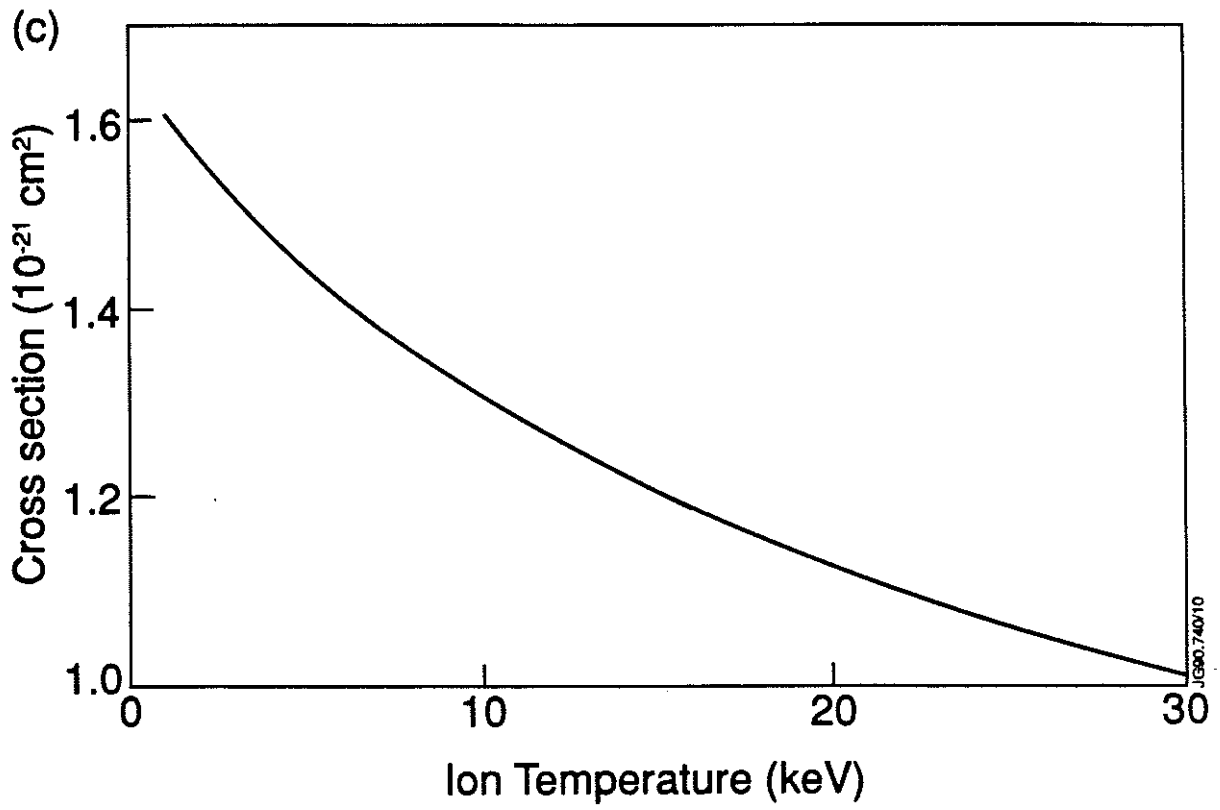

Figure 8 Effect of the energy dependence of the effective charge exchange rate coefficient on the spectral characteristics of the thermal alpha particle spectrum as a function of ion temperature: (a) effect on the deduced temperature for different viewing angles between the viewing line and the neutral beam (E_{beam} = 40 keV/amu, 120° corresponds approximately to the central line of sight of JET multichord system and 150°, to the outermost channel; (b) apparent velocity for a non-rotating plasma (central line of sight); (c) effect on the effective charge exchange rate coefficient (central line of sight).

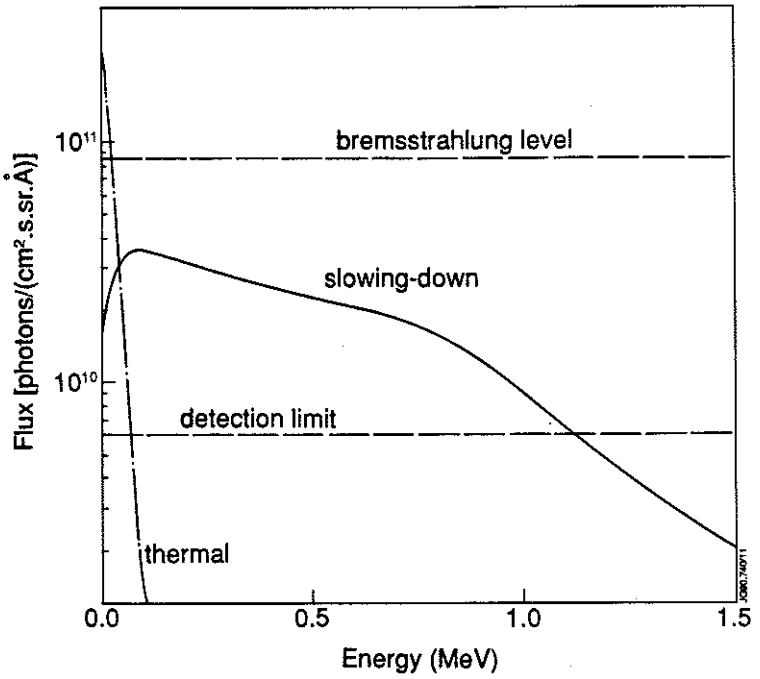

Figure 9 (a) Charge exchange HeII (n=4→3) spectrum expected during the D-T phase of JET plotted in a log/energy plane from thermal and slowing down alpha particles. The simulation uses $N_\alpha = 2x10^{18}$ m^{-3}, $N_e = 5x10^{19}$ m^{-3}, $T_i = 20$ keV, $E_{beam} = 80$ keV/amu, $N_D{}^o \Delta\ell = 7 \times 10^{14}$ m^{-2} and an angle of 60° between the line of sight and the neutral beam (conditions envisaged for alpha particle detection on JET).

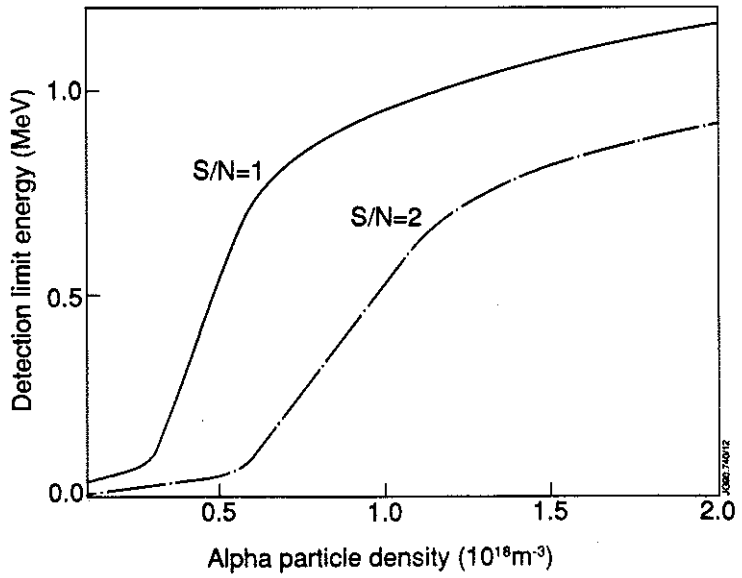

(b) Energy range of detectable slowing down alpha particles for signal to noise ratio ϕ_α/ϕ_{RMS} of 1 and 2 respectively, assuming an integration time of 50 msec and the present JET detector response of 10^7 photons/cm^2.sr. sec./count/sec.

APPENDIX 1.

THE JET TEAM

JET Joint Undertaking, Abingdon, Oxon, OX14 3EA, U.K.

J.M.Adams[1], F.Alladio[4], H.Altmann, R.J.Anderson, G.Appruzzese, W.Bailey, B.Balet, D.V.Bartlett, L.R.Baylor[24], K.Behringer, A.C.Bell, P.Bertoldi, E.Bertolini, V.Bhatnagar, R.J.Bickerton, A.Boileau[3], T.Bonicelli, S.J.Booth, G.Bosia, M.Botman, D.Boyd[31], H.Brelen, H.Brinkschulte, M.Brusati, T.Budd, M.Bures, T.Businaro[4], H.Buttgereit, D.Cacaut, C.Caldwell-Nichols, D.J.Campbell, P.Card, J.Carwardine, G.Celentano, P.Chabert[27], C.D.Challis, A.Cheetham, J.Christiansen, C.Christodoulopoulos, P.Chuilon, R.Claesen, S.Clement[30], J.P.Coad, P.Colestock[6], S.Conroy[13], M.Cooke, S.Cooper, J.G.Cordey, W.Core, S.Corti, A.E.Costley, G.Cottrell, M.Cox[7], P.Cripwell[13], F.Crisanti[4], D.Cross, H.de Blank[16], J.de Haas[16], L.de Kock, E.Deksnis, G.B.Denne, G.Deschamps, G.Devillars, K.J.Dietz, J.Dobbing, S.E.Dorling, P.G.Doyle, D.F.Düchs, H.Duquenoy, A.Edwards, J.Ehrenberg[14], T.Elevant[12], W.Engelhardt, S.K.Erents[7], L.G.Eriksonn[5], M.Evrard[2], H.Falter, D.Flory, M.Forrest[7], C.Froger, K.Fullard, M.Gadeberg[11], A.Galetsas, R.Galvao[8], A.Gibson, R.D.Gill, A.Gondhalekar, C.Gordon, G.Gorini, C.Gormezano, N.A.Gottardi, C.Gowers, B.J.Green, F.S.Griph, M.Gryzinski[26], R.Haange, G.Hammett[6], W.Han[9], C.J.Hancock, P.J.Harbour, N.C.Hawkes[7], P.Haynes[7], T.Hellsten, J.L.Hemmerich, R.Hemsworth, R.F.Herzog, K.Hirsch[14], J.Hoekzema, W.A.Houlberg[24], J.How, M.Huart, A.Hubbard, T.P.Hughes[32], M.Hugon, M.Huguet, J.Jacquinot, O.N.Jarvis, T.C.Jernigan[24], E.Joffrin, E.M.Jones, L.P.D.F.Jones, T.T.C.Jones, J.Källne, A.Kaye, B.E.Keen, M.Keilhacker, G.J.Kelly, A.Khare[15], S.Knowlton, A.Konstantellos, M.Kovanen[21], P.Kupschus, P.Lallia, J.R.Last, L.Lauro-Taroni, M.Laux[33], K.Lawson[7], E.Lazzaro, M.Lennholm, X.Litaudon, P.Lomas, M.Lorentz-Gottardi[2], C.Lowry, G.Magyar, D.Maisonnier, M.Malacarne, V.Marchese, P.Massmann, L.McCarthy[28], G.McCracken[7], P.Mendonca, P.Meriguet, P.Micozzi[4], S.F.Mills, P.Millward, S.L.Milora[24], A.Moissonnier, P.L.Mondino, D.Moreau[17], P.Morgan, H.Morsi[14], G.Murphy, M.F.Nave, M.Newman, L.Nickesson, P.Nielsen, P.Noll, W.Obert, D.O'Brien, J.O'Rourke, M.G.Pacco-Düchs, M.Pain, S.Papastergiou, D.Pasini[20], M.Paume[27], N.Peacock[7], D.Pearson[13], F.Pegoraro, M.Pick, S.Pitcher[7], J.Plancoulaine, J-P.Poffé, F.Porcelli, R.Prentice, T.Raimondi, J.Ramette[17], J.M.Rax[27], C.Raymond, P-H.Rebut, J.Removille, F.Rimini, D.Robinson[7], A.Rolfe, R.T.Ross, L.Rossi, G.Rupprecht[14], R.Rushton, P.Rutter, H.C.Sack, G.Sadler, N.Salmon[13], H.Salzmann[14], A.Santagiustina, D.Schissel[25], P.H.Schild, M.Schmid, G.Schmidt[6], R.L.Shaw, A.Sibley, R.Simonini, J.Sips[16], P.Smeulders, J.Snipes, S.Sommers, L.Sonnerup, K.Sonnenberg, M.Stamp, P.Stangeby[19], D.Start, C.A.Steed, D.Stork, P.E.Stott, T.E.Stringer, D.Stubberfield, T.Sugie[18], D.Summers, H.Summers[20], J.Taboda-Duarte[22], J.Tagle[30], H.Tamnen, A.Tanga, A.Taroni, C.Tebaldi[23], A.Tesini, P.R.Thomas, E.Thompson, K.Thomsen[11], P.Trevalion, M.Tschudin, B.Tubbing, K.Uchino[29], E.Usselmann, H.van der Beken, M.von Hellermann, T.Wade, C.Walker, B.A.Wallander, M.Walravens, K.Walter, D.Ward, M.L.Watkins, J.Wesson, D.H.Wheeler, J.Wilks, U.Willen[12], D.Wilson, T.Winkel, C.Woodward, M.Wykes, I.D.Young, L.Zannelli, M.Zarnstorff[6], D.Zasche[14], J.W.Zwart.

PERMANENT ADDRESS

1. UKAEA, Harwell, Oxon. UK.
2. EUR-EB Association, LPP-ERM/KMS, B-1040 Brussels, Belgium.
3. Institute National des Récherches Scientifique, Quebec, Canada.
4. ENEA-CENTRO Di Frascati, I-00044 Frascati, Roma, Italy.
5. Chalmers University of Technology, Göteborg, Sweden.
6. Princeton Plasma Physics Laboratory, New Jersey, USA.
7. UKAEA Culham Laboratory, Abingdon, Oxon. UK.
8. Plasma Physics Laboratory, Space Research Institute, Sao José dos Campos, Brazil.
9. Institute of Mathematics, University of Oxford, UK.
10. CRPP/EPFL, 21 Avenue des Bains, CH-1007 Lausanne, Switzerland.
11. Risø National Laboratory, DK-4000 Roskilde, Denmark.
12. Swedish Energy Research Commission, S-10072 Stockholm, Sweden.
13. Imperial College of Science and Technology, University of London, UK.
14. Max Planck Institut für Plasmaphysik, D-8046 Garching bei München, FRG.
15. Institute for Plasma Research, Gandhinagar Bhat Gujat, India.
16. FOM Instituut voor Plasmafysica, 3430 Be Nieuwegein, The Netherlands.
17. Commissiariat à L'Energie Atomique, F-92260 Fontenay-aux-Roses, France.
18. JAERI, Tokai Research Establishment, Tokai-Mura, Naka-Gun, Japan.
19. Institute for Aerospace Studies, University of Toronto, Downsview, Ontario, Canada.
20. University of Strathclyde, Glasgow, G4 ONG, U.K.
21. Nuclear Engineering Laboratory, Lapeenranta University, Finland.
22. JNICT, Lisboa, Portugal.
23. Department of Mathematics, Univeristy of Bologna, Italy.
24. Oak Ridge National Laboratory, Oak Ridge, Tenn., USA.
25. G.A. Technologies, San Diego, California, USA.
26. Institute for Nuclear Studies, Swierk, Poland.
27. Commissiariat à l'Energie Atomique, Cadarache, France.
28. School of Physical Sciences, Flinders University of South Australia, South Australia SO42.
29. Kyushi University, Kasagu Fukuoka, Japan.
30. Centro de Investigaciones Energeticas Medioambientales y Techalogicas, Spain.
31. University of Maryland, College Park, Maryland, USA.
32. University of Essex, Colchester, UK.
33. Akademie de Wissenschaften, Berlin, DDR.

CR 88.49.1A